Smart Structures and Systems, *Vol. 23, No. 3 (2019) 215-225*
DOI: https://doi.org/10.12989/sss.2019.23.3.215

Nonlocal strain gradient model for thermal stability of FG nanoplates integrated with piezoelectric layers

Behrouz Karami* and Davood Shahsavari

Department of Mechanical Engineering, Marvdasht Branch, Islamic Azad University, Marvdasht, Iran

(Received May 13, 2018, Revised February 21, 2019, Accepted February 23, 2019)

Abstract. In the present paper, the nonlocal strain gradient refined model is used to study the thermal stability of sandwich nanoplates integrated with piezoelectric layers for the first time. The influence of Kerr elastic foundation is also studied. The present model incorporates two small-scale coefficients to examine the size-dependent thermal stability response. Elastic properties of nanoplate made of functionally graded materials (FGMs) are supposed to vary through the thickness direction and are estimated employing a modified power-law rule in which the porosity with even type of distribution is approximated. The governing differential equations of embedded sandwich piezoelectric porous nanoplates under hygrothermal loading are derived through Hamilton's principle where the Galerkin method is applied to solve the stability problem of the nanoplates with simply-supported edges. It is indicated that the thermal stability characteristics of the porous nanoplates are obviously influenced by the porosity volume fraction and material variation, nonlocal parameter, strain gradient parameter, geometry of the nanoplate, external voltage, temperature and humidity variations, and elastic foundation parameters.

Keywords: porous materials; thermal stability; refined plate theory; nonlocal strain gradient theory; hygrothermal environment; elastic substrate

1. Introduction

FGMs are new types of advanced composite materials in which the properties of the material are varying continuously or exponentially through a direction. Undoubtedly, in the process of making this category of materials, porosities are occurred inside the materials. The researchers have been shown the importance of considering the porosities in the mechanical analysis of FGMs. Hence, a great deal of studies have been conducted to investigate mechanical challenges of these type of materials (see some of the in Refs. (Barati *et al.* 2016, She *et al.* 2018a, She *et al.* 2019, She *et al.* 2018c, Yu *et al.* 2004, Adpakpang *et al.* 2016, Mechab *et al.* 2016, She *et al.* 2018b, Karami and Janghorban 2019, Karami *et al.* 2019b, Karami *et al.*,2018i, Shahsavari *et al.* 2018a, Shahsavari *et al.* 2018c, Shahsavari *et al.* 2018e, Karami *et al.* 2018l, Karami *et al.* 2018k, Ebrahimi *et al.* 2017, Karami *et al.* 2019c)). FGMs also possess amazing features and applications for working in different environmental conditions such as thermal and hygrothermal environments (Lee and Kim 2013, Sobhy 2016). Hence, FGMs have been used in the various engineering fields, notably in high-temperature fields such as thermo-mechanical loading structures, spacecraft, and aircraft, and in nano-electro-mechanical systems (NEMSs) (Li *et al.* 2008, Kar and Panda 2015, Lü *et al.* 2009, Sedighi *et al.* 2015b, Sedighi *et al.* 2015a, Atmane *et al.* 2015, Ghadiri *et al.* 2017, Xiong and Tian 2017, Shafiei and She 2018, She *et al.* 2017, Karami *et al.* 2018c, Karami *et al.* 2018g, Karami *et al.* 2018f, Karami and Karami 2019, Hadji 2017, Saadatfar and Aghaie-Khafri 2015, Zhang and Shi 2010, Barati 2017b, Ghayesh *et al.* 2017c, Ghayesh and Farokhi 2017, Ghayesh *et al.* 2017a, Ghayesh *et al.* 2017b).

Classical theories have increasingly used to study size-independent mechanics of structures in open literature. But, unfortunately, this type of continuum theories is not able to predict the size-dependent behavior of nanostructures. So, to overcome this issue some methods such as molecular dynamic simulation and non-classical continuum theories have been presented so far. (Eringen and Edelen 1972) proposed a model in which small size effects are considered by introducing an additional scale parameter. Therefore, Eringen nonlocal model has been applied to analyze the mechanics of nanoscale structures (Rahmani *et al.* 2017, Bounouara *et al.* 2016, Belkorissat *et al.* 2015, Chaht *et al.* 2015, Ebrahimi and Salari 2017, Bouafia *et al.* 2017, Nejad *et al.* 2016, Nejad and Hadi 2016). Thermal buckling analysis of FG nanosize plates based on trigonometric shear deformation theory is conducted by (Khetir *et al.* 2017). Based on Timoshenko beam theory, (Ebrahimi and Daman 2017) examined dynamic behavior of curved inhomogeneous structures with porosities exposed to thermal environment. Application of nonlocal elasticity theory (NET) in Hygro-thermo-mechanical vibration and buckling analysis of exponentially graded nanoplates resting on elastic foundation was investigated by (Sobhy 2017) based on a refined plate theory. Based on the zeroth-order shear deformation theory, (Bellifa *et al.* 2017) analyzed the nonlinear post-buckling behavior of nanoscale beams using NET of Eringen. Application of two-variable plate theory in forced vibration analysis of single-layer

*Corresponding author, Ph.D. Student
E-mail: behrouz.karami@miau.ac.ir

ISSN: 1738-1584 (Print), 1738-1991 (Online)

graphene sheet under moving load was examined by (Shahsavari and Janghorban 2017). In another work, (Shahsavari *et al.* 2017) proposed a refined four-variable plate model for dynamic analysis of viscoelastic nanoplates under moving load embedded within visco-Pasternak substrate and hygrothermal environment. Free vibration analysis of a piezoelectric nanobeam using NET was carried out by (Kaghazian *et al.* 2017). (Jandaghian and Rahmani, 2017) performed analysis of FG nanobeams based on third-order shear deformation theory under various boundary conditions. Guided wave propagation analysis of fully clamped FG nanoplates with porosities was examined by (Karami *et al.*, 2018a) for the first time. (Karami *et al.* 2019d) presented a nonlocal second-order shear deformation plate theory for thermal stability of sandwich piezoelectric nanoplates with FG core.

As mentioned in pioneer studies, Eringen nonlocal model has only considered stiffness-softening mechanisms of nanostructure systems. Although NET of Eringen is a suitable theory for analyzing of nanostructure, it has some shortcomings due to neglecting stiffness-hardening effect reported in experimental works and strain gradient elasticity (Lam *et al.* 2003). Using nonlocal strain gradient theory (NSGT), (Karami *et al.* 2018h) performed the wave propagation analysis of nanoplates where the results were compared with experimental date for wave frequencies and phase velocities of graphene sheet. They observed that NSGT is more accurate for modeling the nanostructures by considering both stiffness reduction and enhancement effects. In additaion, a large number of studies are performed based on NSGT to analyze the mechanical behavior of nanostructures (Karami and Janghorban 2016, Li and Hu 2015, Şimşek 2016, Shahsavari *et al.* 2018d, Karami *et al.* 2018e, Karami *et al.* 2018j, Karami *et al.* 2018d, Karami *et al.* 2018b, Shahsavari *et al.* 2018b, Karami *et al.* 2019a, She *et al.* 2018d, Nami and Janghorban 2014, Barati 2017a, Barati 2017c, Karami *et al.* 2017, Farajpour *et al.* 2018).

Thermal stability analysis of a sandwich nanoplates integrated with piezoelectric layers is investigated here using nonlocal strain gradient refined plate model for the first time. The core of the sandwich plate is considered as an FGMs in which the porosities effects is also studied. The porosity-dependent material properties of such structure are modeled via a modified power-law rule. The governing equations of motion as well as classical and non-classical boundary conditions related are obtained through a virtual work of the Hamiltonian principles where the Galerkin procedure is performed to solve the stability phenomena of a simply supported nanoplates. The influences of material composition, porosities, external voltage, temperature and humidity differences, small-scale parameter, geometrical parameters and elastic Kerr foundation on thermal stability characteristics of nanoplate is presented afterward in a parametric study.

2. Nonlocal strain gradient nanoplate model

Nonlocal strain gradient elasticity (Lim *et al.* 2015) enumerates the stress for both nonlocal stress and strain fields. Therefore, the stress can be expressed by

$$\sigma_{ij} = \sigma_{ij}^{(0)} - \nabla \partial \sigma_{ij}^{(1)} \tag{1}$$

in which $\sigma_{ij}^{(0)}$ and $\sigma_{ij}^{(1)}$ are related to strain ε_{ij} and strain gradient $\nabla\varepsilon_{ij}$, respectively and are defined as

$$\sigma_{ij}^{(0)} = \int_0^L C_{ijkl}\alpha_0(x,x',e_0a)\varepsilon'_{kl}(x')dx' \tag{2}$$

$$\sigma_{ij}^{(1)} = l^2\int_0^L C_{ijkl}\alpha_1(x,x',e_1a)\nabla\varepsilon'_{kl}(x')dx' \tag{3}$$

where C_{ijkl} are the elastic constants and e_0a and e_1a consider the influence of nonlocal stress field and l is the strain gradient parameter which defines the effects of higher order strain gradient stress field. When the nonlocal functions $\alpha_0(x,x',e_0a)$ and $\alpha_0(x,x',e_1a)$ satisfy the developed conditions by Eringen, the constitutive relation of NSGT has the following form

$$\begin{aligned}&\left[1-(e_1a)^2\nabla^2\right]\left[1-(e_0a)^2\nabla^2\right]\sigma_{ij}\\&=C_{ijkl}\left[1-(e_1a)^2\nabla^2\right]\varepsilon_{kl}-C_{ijkl}l^2\left[1-(e_0a)^2\nabla^2\right]\nabla^2\varepsilon_{kl}\end{aligned} \tag{4}$$

where ∇^2 is Laplacian operator in Cartesian coordinates. Supposing e_1=e_0=e and discarding terms of order $O(\nabla^2)$, the general constitutive relation in Eq. (4) can be rewritten as (Lim *et al.* 2015)

$$\left[1-(ea)^2\nabla^2\right]\sigma_{ij} = C_{ijkl}\left[1-l^2\nabla^2\right]\varepsilon_{kl} \tag{5}$$

The following equation can be used to include the influences of hygro-thermal loading and piezoelectric layers in the Eq. (5).

$$\begin{aligned}&(1-\mu\nabla^2)\sigma_{ij} = C_{ijkl}\left[(1-\lambda\nabla^2)\varepsilon_{kl}-\alpha_{ij}\Delta\mathrm{T}-\beta_{ij}\Delta\mathrm{H}\right]\\&-[e]\{E\}\end{aligned} \tag{6}$$

in which $\lambda = l^2$ and $\mu = (ea)^2$; [e] is the piezoelectric constants matrix; $\{E\}$ is the electric field intensity vector; α_{ij} is thermal coefficient; β_{ij} is moisture coefficient. The equivalent form of Eq. (6) is presented as

$$\mathrm{L}_\mu\sigma_{ij} = C_{ijkl}\left[\mathrm{L}_l\varepsilon_{kl}-\alpha_{ij}\Delta\mathrm{T}-\beta_{ij}\Delta\mathrm{H}\right]-[e]\{E\} \tag{7}$$

where the linear operators are defined as

$$\mathrm{L}_\mu = (1-\mu\nabla^2), \mathrm{L}_l = (1-\lambda\nabla^2) \tag{8}$$

The stiffness e_{31}, e_{32}, e_{24}, e_{25} can be considered as the following forms with respect to dielectric constants d_{31}, d_{32}, d_{24}, d_{15} and elastic stiffness C_{ij} of piezoelectric actuator layers (Karami *et al.* 2019d).

$$\begin{aligned}&e_{31} = d_{31}C_{11}^a + d_{32}C_{12}^a, e_{32} = d_{31}C_{12}^a + d_{32}C_{22}^a\\&e_{24} = d_{24}C_{44}^a, e_{15} = d_{15}C_{55}^a\end{aligned} \tag{9}$$

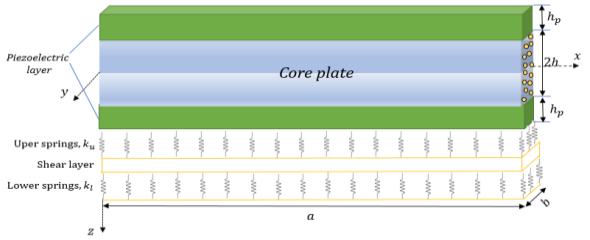

Fig. 1 Geometry of Kerr elastic substrate with piezoelectric layers at top and bottom surfaces

Note: in the current study to applying the external voltage on the mechanics of the sandwich plate, the following relation is assumed

$$E_z = V_p / h_p \,,\; E_x = E_y = 0 \tag{10}$$

in which V_p denotes the voltage applied to the actuators in the thickness direction.

3. Theory and formulation

A sandwich piezoelectric nanoplate with FG core as shown in Fig. 1 according to coordinate system (x, y, z) that a is length, b is width is assumed. The thickness of elastic core is $2h$ and thickness of each piezoelectric layer is h_p.

3.1 Displacement and strain

With regard to the plate theories, the four variable refined model initially proposed by Shimpi (Shimpi 2002) is widely considered as a reliable theory in which no shear correction factor is required. In Shimpi's theory, the displacement field is defined as

$$u(x,y,z,t) = u_0(x,y,t) - z\frac{\partial w_b}{\partial x} - f(z)\frac{\partial w_s}{\partial x} \tag{11}$$

$$v(x,y,z,t) = v_0(x,y,t) - z\frac{\partial w_b}{\partial y} - f(z)\frac{\partial w_s}{\partial y} \tag{12}$$

$$w(x,y,z,t) = w_b(x,y,t) + w_s(x,y,t) \tag{13}$$

in which u_0 and v_0 denote in-plane displacments and w_b and w_s denote the bending and shear transverse displacement, respectively. The shape function of transverse shear deformation is considered as

$$f(z) = -z/4 + 5z^3/3h^2 \tag{14}$$

According to the displacement field which is presented in Eqs. (11)-(13), the following nonzero strain expressions can be obtained as

$$\begin{Bmatrix}\varepsilon_x\\ \varepsilon_y\\ \gamma_{xy}\end{Bmatrix} = \begin{Bmatrix}\varepsilon_x^0\\ \varepsilon_y^0\\ \gamma_{xy}^0\end{Bmatrix} + z\begin{Bmatrix}K_x^b\\ K_y^b\\ K_{xy}^b\end{Bmatrix} + f\begin{Bmatrix}K_x^s\\ K_y^s\\ K_{xy}^s\end{Bmatrix}$$
$$\begin{Bmatrix}\gamma_{yz}\\ \gamma_{xz}\end{Bmatrix} = g\begin{Bmatrix}\gamma_{yz}^s\\ \gamma_{xz}^s\end{Bmatrix},\; g = 1 - \frac{\partial f}{\partial z} \tag{15}$$

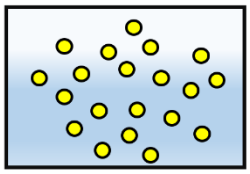

Fig. 2 Porosity model of FGM.

where

$$\begin{Bmatrix}\varepsilon_x^0\\ \varepsilon_y^0\\ \gamma_{xy}^0\end{Bmatrix} = \begin{Bmatrix}\frac{\partial u_0}{\partial x}\\ \frac{\partial v_0}{\partial y}\\ \frac{\partial u_0}{\partial y} + \frac{\partial v_0}{\partial x}\end{Bmatrix}, \begin{Bmatrix}k_x^b\\ k_y^b\\ k_{xy}^b\end{Bmatrix} = \begin{Bmatrix}-\frac{\partial^2 w_b}{\partial x^2}\\ -\frac{\partial^2 w_b}{\partial y^2}\\ -2\frac{\partial^2 w_b}{\partial x\,\partial y}\end{Bmatrix}$$
$$\begin{Bmatrix}k_x^s\\ k_y^s\\ k_{xy}^s\end{Bmatrix} = \begin{Bmatrix}-\frac{\partial^2 w_s}{\partial x^2}\\ -\frac{\partial^2 w_s}{\partial y^2}\\ -2\frac{\partial^2 w_s}{\partial x\,\partial y}\end{Bmatrix}, \begin{Bmatrix}\gamma_{xz}^s\\ \gamma_{yz}^s\end{Bmatrix} = \begin{Bmatrix}\frac{\partial w_s}{\partial x}\\ \frac{\partial w_s}{\partial y}\end{Bmatrix} \tag{16}$$

3.2 Constitutive equations

In the present work, FGMs with varying material properties along the thickness direction as well as an even type of porosity distribution effect are considred. To estimate the prosity-dependent material propetries, a modefied power-law rule is used sa follows (Wattanasakulpong and Ungbhakorn 2014)

$$P(z,\xi) = P_B + (P_T - P_B)\left(\frac{1}{2} - \frac{z}{2h}\right)^n - \frac{\xi}{2}(P_T + P_B) \tag{17}$$

in which n indicates the power-law index; P_T and P_B denote, respectively, the material properties of the top and the bottom faces of the graded structures; $\xi(\xi << 0)$ is the porosity coefficient (volume fraction of porosities). The distribution of the even porosity distribution is shown in Fig. 2. The material properties such as Young's modulus E, Poisson's ratio v, thermal and moisture expansion coefficients (α and β), shear modulus G, and mass density ρ are estimated through the Eq. (17).

3.3 Governing equations

The extended Hamilton principle express that

$$\int_0^t \delta(U + V)dt = 0 \tag{18}$$

where U is strain energy and V is work done by external (applied) forces. The first variation of strain energy can be concluded as

$$\delta U = \int_V \left[\sigma_{xx}\delta\varepsilon_{xx} + \sigma_{yy}\delta\varepsilon_{yy} + \tau_{yz}\delta\gamma_{yz} + \tau_{xz}\delta\gamma_{xz} + \tau_{xy}\delta\gamma_{xy}\right]dV$$
$$= \int_0^L \left[N_x\delta\varepsilon_x^0 + N_y\delta\varepsilon_y^0 + N_{xy}\delta\gamma_{xy}^0 + M_x^b\delta k_x^b + M_y^b\delta k_y^b + M_{xy}^b\delta k_{xy}^b\right.$$
$$\left. + M_x^s\delta k_x^s + M_y^s\delta k_y^s + M_{xy}^s\delta k_{xy}^s + Q_{yz}^s\gamma_{yz}^0 + Q_{xz}^s\gamma_{xz}^0\right]dx = 0 \tag{19}$$

The first variation of work done by applied forces can be stated as

$$\delta V = \int_0^L \Big[N_x^0 \frac{\partial(w_b+w_s)}{\partial x}\frac{\partial\delta(w_b+w_s)}{\partial x} + N_y^0 \frac{\partial(w_b+w_s)}{\partial y}\frac{\partial\delta(w_b+w_s)}{\partial y} + 2\delta N_{xy}^0 \frac{\partial(w_b+w_s)}{\partial x}\frac{\delta(w_b+w_s)}{\partial y} + (N^T+N^H)\Big(\frac{\partial w}{\partial x}\frac{\partial\delta w}{\partial x}+\frac{\partial w}{\partial y}\frac{\partial\delta w}{\partial y}\Big) + q_{\text{Kerr}}\delta w \Big] = 0 \tag{20}$$

where N_x^0, N_y^0 and N_{xy}^0 are in-plane applied loads (buckling loads); the external forces N^T and N^H according to the changes of temperature and moisture in core are expressed as

$$N^T = \int_{-h}^{h} E(z)\alpha(z)(\Delta T)\mathrm{d}z \tag{21}$$

$$N^H = \int_{-h}^{h} E(z)\beta(z)(\Delta H)\mathrm{d}z \tag{22}$$

in which $\Delta T = T - T_0$ and $\Delta H = H - H_0$ where T_0 and H_0 can be introduced as the reference temperature and moisture, respectively. The external transverse forces q_{Kerr} caused by elastic medium are represented in terms of displacements as (Kneifati 1985)

$$q_{\text{Kerr}} - \left(\frac{k_s}{k_l+k_u}\right)\nabla^2 q_{\text{Kerr}} = \left(\frac{k_l k_u}{k_l+k_u}\right)w - \left(\frac{k_s k_u}{k_l+k_u}\right)\nabla^2 w \tag{23}$$

in which k_l, k_u and k_s are the stiffness of upper and lower springs and shear layer, respectively. The following Euler–Lagrange equations are obtained by inserting Eqs. (19) and (20) in Eq. (18) when the coefficients of δu_0, δv_0, δw_b and δw_s are equal to zero

$$\frac{\partial N_x}{\partial x} + \frac{\partial N_{xy}}{\partial y} = 0 \tag{24}$$

$$\frac{\partial N_{xy}}{\partial x} + \frac{\partial N_y}{\partial y} = 0 \tag{25}$$

$$\begin{aligned} &\frac{\partial^2 M_x^b}{\partial x^2} + 2\frac{\partial^2 M_{xy}^b}{\partial x\,\partial y} + \frac{\partial^2 M_y^b}{\partial y^2} - \Big(\frac{k_l k_u}{k_l+k_u}\Big)w \\ &+\Big(\frac{k_s k_u}{k_l+k_u} + N^T + N^H\Big)\nabla^2 w \\ &N_x^0\frac{\partial^2 w}{\partial x^2} + N_y^0\frac{\partial^2 w}{\partial x^2} + 2N_{xy}^0\frac{\partial^2 w}{\partial x\,\partial y} = 0 \end{aligned} \tag{26}$$

$$\begin{aligned} &\frac{\partial^2 M_x^s}{\partial x^2} + 2\frac{\partial^2 M_{xy}^s}{\partial x\,\partial y} + \frac{\partial^2 M_y^s}{\partial y^2} + \frac{\partial Q_{xz}^s}{\partial x} + \frac{\partial Q_{yz}^s}{\partial y} \\ &-\Big(\frac{k_l k_u}{k_l+k_u}\Big)(w_b+w_s) + \Big(\frac{k_s k_u}{k_l+k_u} + N^T + N^H\Big)\nabla^2 w \\ &N_x^0\frac{\partial^2 w}{\partial x^2} + N_y^0\frac{\partial^2 w}{\partial x^2} + 2N_{xy}^0\frac{\partial^2 w}{\partial x\,\partial y} = 0 \end{aligned} \tag{27}$$

where N, M, and Q are the stress resultants and can be defined as follows

$$\begin{Bmatrix}\{N\}\\ \{M^b\}\\ \{M^s\}\end{Bmatrix} = \begin{bmatrix}[A] & [B] & [B^s]\\ [B] & [D] & [D^s]\\ [B^s] & [D^s] & [H^s]\end{bmatrix}\begin{Bmatrix}\varepsilon^0\\ k^b\\ k^s\end{Bmatrix}$$
$$\begin{Bmatrix}\{Q_{xz}\}\\ \{Q_{yz}\}\end{Bmatrix} = \begin{bmatrix}A_{44}^s & 0\\ 0 & A_{55}^s\end{bmatrix}\begin{Bmatrix}\gamma_{xz}^s\\ \gamma_{Yz}^s\end{Bmatrix} \tag{28}$$

in which

$$(A,B,B^s,D,D^s,H^s) = \int_{-h-h_p}^{h+h_p} C_{ij}(1,z,f,z^2,zf,f^2)dz \tag{29}$$

and

$$A_{44}^s = A_{55}^s = \int_{-h-h_p}^{h+h_p} C_{44}g^2 dz \tag{30}$$

The classical and non-classical boundary conditions can be obtained in the derivation process when using the integrations by parts. Thus, we obtain classical boundary conditions at x=0 or a and y=0 or b as (Barati 2018)

$$\begin{aligned} &\text{Specify } w_b \text{ or } \left(\frac{\partial M_x^b}{\partial x}+\frac{\partial M_{xy}^b}{\partial y}\right)n_x + \left(\frac{\partial M_y^b}{\partial y}+\frac{\partial M_{xy}^b}{\partial x}\right)n_y = 0\\ &\text{Specify } w_s \text{ or } \left(\frac{\partial M_x^s}{\partial x}+\frac{\partial M_{xy}^s}{\partial y}+Q_{xz}\right)n_x + \left(\frac{\partial M_y^s}{\partial y}+\frac{\partial M_{xy}^s}{\partial x}+Q_{yz}\right)n_y = 0\\ &\text{Specify } \frac{\partial w_b}{\partial n} \text{ or } M_x^b n_x^2 + n_x n_y M_{xy}^b + M_y^b n_y^2 = 0 \end{aligned} \tag{31}$$

in which $\frac{\partial()}{\partial n} = n_x\frac{\partial()}{\partial x} + n_y\frac{\partial()}{\partial y}$; n_x and n_y denote the x and y-components of the unit normal vector on the nanoplate boundaries, respectively and the non-classical boundary conditions are

$$\begin{aligned} &\text{Specify } \frac{\partial^2 w_b}{\partial x^2} \text{ or } M_x^b = 0, \text{ Specify } \frac{\partial^2 w_b}{\partial y^2} \text{ or } M_y^b = 0\\ &\text{Specify } \frac{\partial^2 w_s}{\partial x^2} \text{ or } M_x^s = 0, \text{ Specify } \frac{\partial^2 w_s}{\partial y^2} \text{ or } M_y^s = 0 \end{aligned} \tag{32}$$

3.3 Equations of motion in terms of displacements

On the basis of the nonlocal strain gradient theory, the constitutive relations of presented nanoplate can be stated as

$$\begin{aligned} \mathrm{L}_\mu\begin{bmatrix}\sigma_x\\ \sigma_y\\ \tau_{xz}\\ \tau_{yz}\\ \tau_{xy}\end{bmatrix} &= \begin{bmatrix}C_{11} & C_{12} & 0 & 0 & 0\\ C_{12} & C_{22} & 0 & 0 & 0\\ 0 & 0 & C_{44} & 0 & 0\\ 0 & 0 & 0 & C_{55} & 0\\ 0 & 0 & 0 & 0 & C_{66}\end{bmatrix} \times \left\langle \mathrm{L}_l\begin{bmatrix}\varepsilon_x\\ \varepsilon_y\\ \gamma_{xz}\\ \gamma_{yz}\\ \gamma_{xy}\end{bmatrix} - \alpha\Delta T - \beta\Delta H \right\rangle \\ &- \begin{bmatrix}0 & 0 & e_{31}\\ 0 & 0 & e_{32}\\ 0 & e_{24} & 0\\ e_{15} & 0 & 0\end{bmatrix}\begin{Bmatrix}E_x\\ E_y\\ E_z\end{Bmatrix} \end{aligned} \tag{33}$$

in which $(\sigma_x,\sigma_y,\tau_{yz},\tau_{xz},\tau_{xy})$ and $(\varepsilon_x,\varepsilon_y,\gamma_{yz},\gamma_{xz},\gamma_{xy})$ denote the stress and strain components, respectively. Elastic constants of FGM layer can be defined as

$$C_{11}=C_{22}=\frac{E(z)}{\left(1-\nu^2\right)},C_{12}=\nu C_{11}$$
$$C_{44}=C_{55}=C_{66}=\frac{E(z)}{2(1+\nu)} \tag{34}$$

Using Eqs. (24)-(27), and also with consideration Eq. (33) the nonlocal strain gradient equations of motion can be expressed in terms of displacements as

$$\begin{aligned}
&\mathrm{L}_l\left\{A_{11}\frac{\partial^2 u_0}{\partial x^2}+A_{66}\frac{\partial^2 u_0}{\partial y^2}+(A_{12}+A_{66})\frac{\partial^2 v_0}{\partial x\,\partial y}\right\}\\
&+\mathrm{L}_l\left\{-B_{11}\frac{\partial^3 w_b}{\partial x^3}-(B_{12}+2B_{66})\frac{\partial^3 w_b}{\partial x\,\partial y^2}-B_{11}^s\frac{\partial^3 w_s}{\partial x^3}\right\}\\
&+\mathrm{L}_l\left\{-(B_{12}^s+2B_{66}^s)\frac{\partial^3 w_s}{\partial x\,\partial y^2}\right\}+\mathrm{L}_\mu\left\{-\frac{\partial}{\partial x}J_1\right\}=0
\end{aligned} \tag{35}$$

$$\begin{aligned}
&\mathrm{L}_l\left\{A_{66}\frac{\partial^2 v_0}{\partial x^2}+A_{22}\frac{\partial^2 v_0}{\partial y^2}+(A_{12}+A_{66})\frac{\partial^2 u_0}{\partial x\,\partial y}\right\}\\
&+\mathrm{L}_l\left\{-B_{22}\frac{\partial^3 w_b}{\partial y^3}-(B_{12}+2B_{66})\frac{\partial^3 w_b}{\partial x^2\partial y}-B_{22}^s\frac{\partial^3 w_s}{\partial x^3}\right\}\\
&+\mathrm{L}_l\left\{-(B_{12}^s+2B_{66}^s)\frac{\partial^3 w_s}{\partial x^2\partial y}\right\}+\mathrm{L}_\mu\left\{-\frac{\partial}{\partial y}J_4\right\}=0
\end{aligned} \tag{36}$$

$$\begin{aligned}
&\mathrm{L}_l\left\{B_{11}\frac{\partial^3 u_0}{\partial x^3}+(B_{12}+2B_{66})\frac{\partial^3 u_0}{\partial x\,\partial y^2}+(B_{12}+2B_{66})\frac{\partial^3 v_0}{\partial x^2\partial y}\right\}\\
&+\mathrm{L}_l\left\{+B_{22}\frac{\partial^3 v_0}{\partial y^3}-D_{11}\frac{\partial^4 w_b}{\partial x^4}-2(D_{12}+2D_{66})\frac{\partial^4 w_b}{\partial x^2\partial y^2}\right\}\\
&+\mathrm{L}_l\left\{-D_{22}\frac{\partial^4 w_b}{\partial x^4}-D_{11}^s\frac{\partial^4 w_s}{\partial x^4}-2(D_{12}^s+2D_{66}^s)\frac{\partial^4 w_s}{\partial x^2\partial y^2}\right\}\\
&+\mathrm{L}_l\left\{-D_{22}^s\frac{\partial^4 w_s}{\partial y^4}\right\}+\mathrm{L}_\mu\left\{-\left(\frac{k_l k_u}{k_l+k_u}\right)(w_b+w_s)\right\}\\
&+\mathrm{L}_\mu\left\{\left(\frac{k_s k_u}{k_l+k_u}\nabla^2(w_b+w_s)+(N^{\mathrm{T}}+N^{\mathrm{H}})\nabla^2(w_b+w_s)\right)\right\}\\
&+\mathrm{L}_\mu\left\{N_x^0\frac{\partial^2(w_b+w_s)}{\partial x^2}+N_y^0\frac{\partial^2(w_b+w_s)}{\partial x^2}\right\}\\
&+\mathrm{L}_\mu\left\{2N_{xy}^0\frac{\partial^2(w_b+w_s)}{\partial x\,\partial y}-\frac{\partial^2}{\partial x^2}J_2-\frac{\partial^2}{\partial y^2}J_5\right\}=0
\end{aligned} \tag{37}$$

$$\begin{aligned}
&\mathrm{L}_l\left\{B_{11}^s\frac{\partial^3 u_0}{\partial x^3}+(B_{12}^s+2B_{66}^s)\frac{\partial^3 u_0}{\partial x\,\partial y^2}+(B_{12}^s+2B_{66}^s)\frac{\partial^3 v_0}{\partial x^2\partial y}\right\}\\
&+\mathrm{L}_l\left\{B_{22}\frac{\partial^3 v_0}{\partial y^3}-D_{11}^s\frac{\partial^4 w_b}{\partial x^4}+A_{55}^s\frac{\partial^2 w_s}{\partial x^2}+A_{44}^s\frac{\partial^2 w_s}{\partial y^2}\right\}\\
&+\mathrm{L}_l\left\{-2(D_{12}^s+2D_{66}^s)\frac{\partial^4 w_b}{\partial x^2\partial y^2}-D_{22}^s\frac{\partial^4 w_b}{\partial x^4}-H_{11}^s\frac{\partial^4 w_s}{\partial x^4}\right\}\\
&+\mathrm{L}_l\left\{-2(H_{12}^s+2H_{66}^s)\frac{\partial^4 w_s}{\partial x^2\partial y^2}-H_{22}^s\frac{\partial^4 w_s}{\partial y^4}\right\}\\
&+\mathrm{L}_\mu\left\{-\left(\frac{k_l k_u}{k_l+k_u}\right)(w_b+w_s)+\left(\frac{k_s k_u}{k_l+k_u}\right)\nabla^2(w_b+w_s)\right\}\\
&+\mathrm{L}_\mu\left\{(N^{\mathrm{T}}+N^{\mathrm{H}})\nabla^2(w_b+w_s)+N_x^0\frac{\partial^2(w_b+w_s)}{\partial x^2}\right\}\\
&+\mathrm{L}_\mu\left\{N_y^0\frac{\partial^2(w_b+w_s)}{\partial x^2}+2N_{xy}^0\frac{\partial^2(w_b+w_s)}{\partial x\,\partial y}\right\}\\
&+\mathrm{L}_\mu\left\{-\frac{\partial^2}{\partial x^2}J_3-\frac{\partial^2}{\partial y^2}J_6\right\}=0
\end{aligned} \tag{38}$$

where

$$\begin{aligned}
(J_1,J_2,J_3)&=\int_{-\frac{h}{2}-h_p}^{\frac{h}{2}+h_p}e_{31}E_z(1,z,f)\\
(J_4,J_5,J_6)&=\int_{-\frac{h}{2}-h_p}^{\frac{h}{2}+h_p}e_{32}E_z(1,z,f)
\end{aligned} \tag{39}$$

4. Solution procure

The Galerkin method is an efficient semi-analytical-numerical tool for solving the partial differential equations. In present solution technique, the displacement field can be deliberated as (Barati 2018)

$$u=\sum_{m=1}^{\infty}\sum_{n=1}^{\infty}U_{mn}\frac{\partial X_m(x)}{\partial x}Y_n(y) \tag{40}$$

$$v=\sum_{m=1}^{\infty}\sum_{n=1}^{\infty}V_{mn}X_m(x)\frac{\partial Y_n(y)}{\partial y} \tag{41}$$

$$w_b=\sum_{m=1}^{\infty}\sum_{n=1}^{\infty}W_{bmn}X_m(x)Y_n(y) \tag{42}$$

$$w_s=\sum_{m=1}^{\infty}\sum_{n=1}^{\infty}W_{smn}X_m(x)Y_n(y) \tag{43}$$

where (U_{mn}, V_{mn}, W_{bmn}, W_{smn}) are the unknown coefficients and the functions; X_m and Y_n satisfies the boundary conditions. The function X_m for simply-supported boundary conditions is defined by

$$\begin{aligned}
X_m&=\sin(\lambda_m x)\\
\lambda_m&=\frac{m\pi}{a}
\end{aligned} \tag{44}$$

The classical and non-classical boundary condition based on the present plate model are (Barati 2018)

$$\begin{aligned}
&w_b=w_s=0\\
&\frac{\partial^2 w_b}{\partial x^2}=\frac{\partial^2 w_s}{\partial x^2}=\frac{\partial^2 w_b}{\partial y^2}=\frac{\partial^2 w_s}{\partial y^2}=0\\
&\frac{\partial^4 w_b}{\partial x^4}=\frac{\partial^4 w_s}{\partial x^4}=\frac{\partial^4 w_b}{\partial y^4}=\frac{\partial^4 w_s}{\partial y^4}=0
\end{aligned} \tag{45}$$

By substituting Eqs. (40)-(43) into Eqs. (35)-(38), one can write these four equations in matrix format to find the critical buckling temperature. In this paper, uniform type of temperature distributions is considered. It is assumed that the FG nanoplate is under constant temperature and then the FG nanoplate is exposed to a constant temperature rise such that the FG nanoplate buckles. By solving the above equations, the results for the thermal stability of sandwich porous nanoplates subjected to uniform temperature distribution can be obtained.

Table 1 Comparison of critical buckling temperature $(\Delta\bar{T}_{cr})$ of FG nanoplate for various gradient index and nonlocal parameters (a/h=10)

μ	n=0		n=0.2		n=1		n=5	
	SSDT*	Present	SSDT*	Present	SSDT*	Present	SSDT*	Present
1	10.0931	10.5926	7.1724	7.6980	4.5418	5.1729	4.0601	4.8376
2	8.6647	9.0936	6.1573	6.6085	3.8991	4.4409	3.4855	4.1530
3	7.5905	7.9662	5.3940	5.7892	3.4157	3.8903	3.0534	3.6381
4	6.7532	7.0875	4.7990	5.1507	3.0389	3.4612	2.7166	3.2368

*SSDT: (Karami *et al.* 2019d)

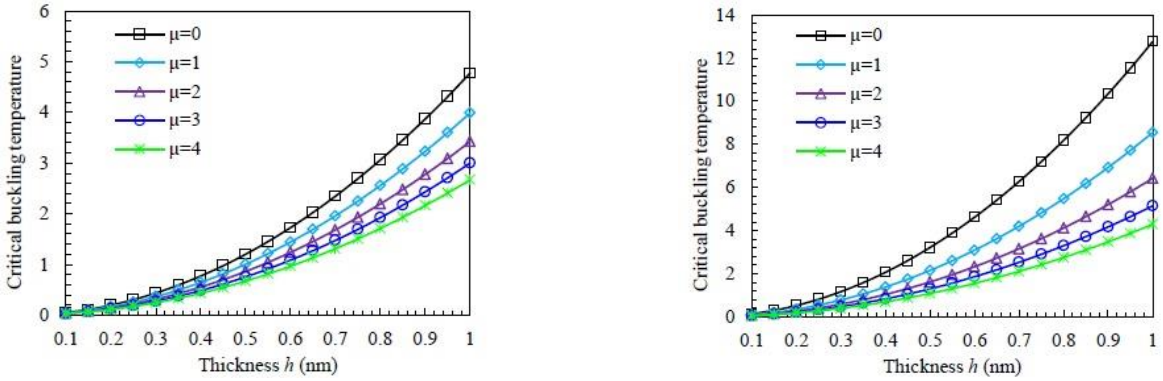

(a) a/b=1 (b) a/b=2

Fig. 3 Variation of critical buckling temperature under nonlocal parameter versus thickness of FG nanoplate

5. Numerical results

In this paper, the nonlocal strain gradient response of thermal stability of sandwich piezoelectric nanoplates with porous core embedded on an elastic medium under hygrothermal environment effects is investigated using a refined higher-order plate theory with presenting the Galerkin solution for the first time. The porosity-dependent material properties of FG nanoplate are assumed to vary gradually along the thickness through the modified power-law rule. The sandwich piezoelectric nanoplate is composed of Aluminum E_b=70GPa, ν_b=0.3 α_b=23×10^{-6}1/K,β_b = 0.44 (wt.%H_2O)$^{-1}$ and Alumina E_t=380GPa, ν_t=0.3, α_t=7×10^{-6}1/K,β_t = 0.001 (wt.%H_2O)$^{-1}$ for the FGM substrate, and G-1195 N for the piezoelectric layers. Thickness of actuator layer is $h_a = 2\times10^{-12}$ m and properties of G-1195 N are $E_{11} = E_{22} = 63\times10^9$ pa $d_{31} = d_{32} = 1\times10^{-13}$ m/V . A three parameters elastic foundation including the upper and lower linear springs along with the shear layer is in contact with the plate. In this study, various non-dimensional parameters are used as follows:

$$\Delta\bar{T}_{cr} = 1000\alpha_c \times \Delta T, K_l = \frac{k_l a^4}{D_{11}}, K_u = \frac{k_u a^4}{D_{11}}, K_s = \frac{k_s a^2}{D_{11}}$$

$$D_{11} = (E_m h^3)/(12(1-\nu_m^2))$$

Table 1 presents the comparison results for a FG nanoplate for various gradient index and nonlocal parameters and good agreement is observed.

Figs. 3 and 4 present the variation of critical buckling temperature of simply-supported porous nanoplate respectively versus nonlocal parameter (μ) and strain gradient length scale parameter (λ) for varying thickness between h=0.1-1.0 nm for different aspect ratios (a/b) at length of plate a=10 nm, gradient index n=1, porosity coefficient ξ=0.2. It is evident that for all values of nonlocality parameters, increasing thickness value (h) leads to higher dimensionless buckling loads. Furthermore, it is interesting to point out that that the effect of nonlocal parameter and strain gradient length scale parameter on porous nanoplates with the higher aspect ratio is more significant than that of with lower aspect ratio. Therefore, effect of scale parameters on thermal stability of porous nanoplates depends on the value of length-to-thickness and width-to-length ratios.

The effect of external voltage on the thermal stability of the porous nanoplate can also be investigated. Shown in Figs. 5 and 6 are the critical buckling temperature of the sandwich piezoelectric nanoplate with porous core in terms of the voltage rising for different aspect ratios where a/h= 10, n=1, ξ=0.2. The obtained results indicate that with increasing voltage, the critical buckling of the FG nanoplate is decreased for all nonlocal and strain gradient length scale parameters. Also, an increase in the nonlocal and strain grained length scale parameters leads to smaller and greater

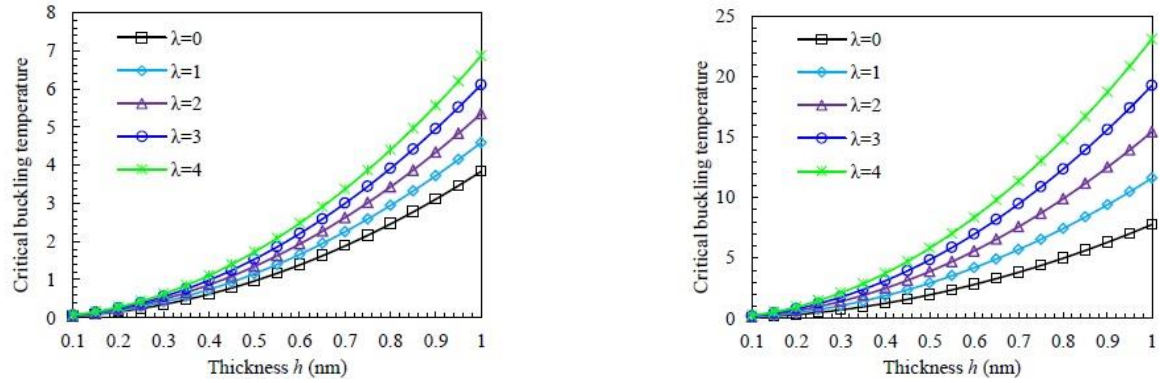

(a) a/b=1 (b) a/b=2

Fig. 4 Variation of critical buckling temperature under strain gradient length scale parameter versus thickness of FG nanoplate

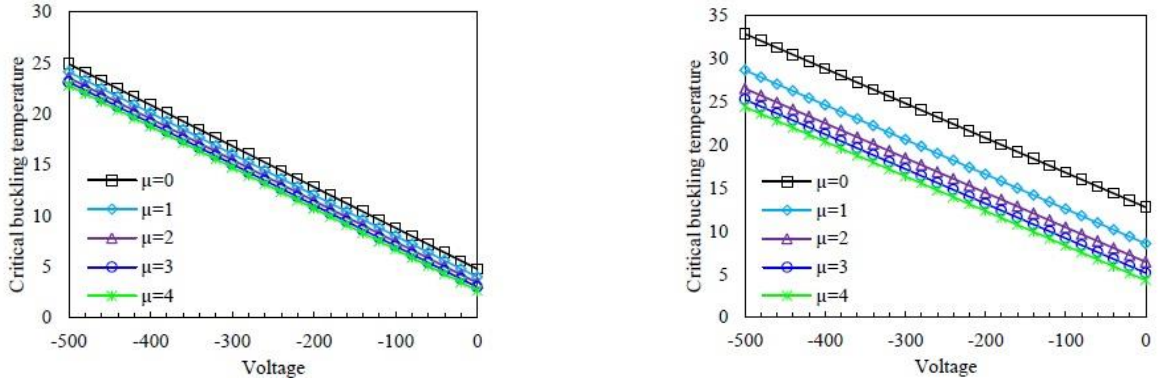

(a) a/b=1 (b) a/b=2

Fig. 5 The effects of voltage and nonlocal parameter on critical buckling temperature for different aspect ratio

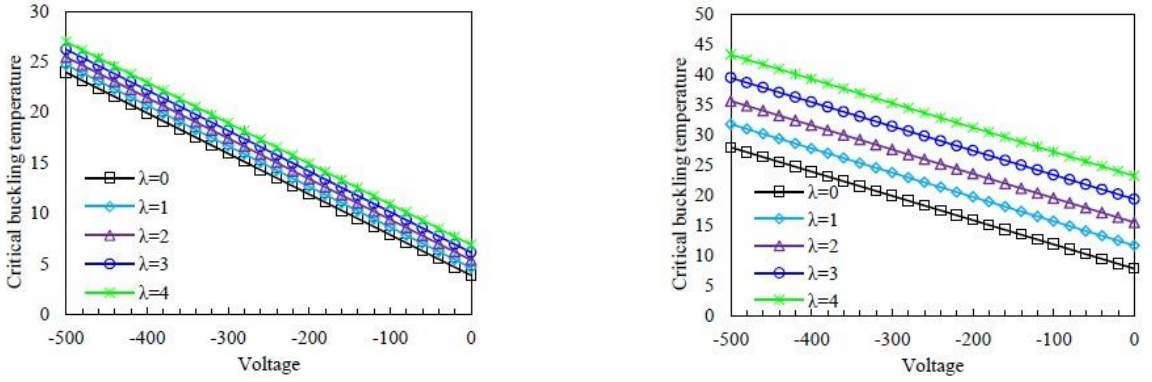

(a) a/b=1 (b) a/b=2

Fig. 6 The effects of voltage and strain gradient length scale parameter on critical buckling temperature for different aspect ratio

critical buckling temperature, respectively. It is also observed that thermal stability response of FG nanoplate is influenced significantly by scale parameters under voltage differences so that it is more sensitive at higher aspect ratios.

Fig. 7 and 8 indicate the effects of material composition, and small scale parameters on the critical buckling temperature of porous nanoplates where ξ=0.2. One particularly key fact highlighted by these figures is that the critical buckling temperature reduces as the gradient index increases, especially for lower gradient indices. It is because higher portion of metallic phase leads to the higher gradient index. In addition, it should be noted that μ=0 and λ=0 corresponds to local plate model. The increase in nonlocal parameter (μ) causes to reduction in the critical buckling temperature. The reason is softening impact of nonlocal

parameter on the nanoplate rigidity. But, strain gradient length scale parameter (λ) has an increasing effect on the nanoplate stiffness and critical buckling temperate. So, both scale parameters have significant effect on the thermal stability response of porous nanoplates and should be considered for their accurate analysis.

To study the environmental effect on the thermal stability of porous nanoplate, effects of temperature and moisture differences on the critical buckling temperature with respect to nonlocal parameter (μ) and strain gradient length scale parameter (λ) are demonstrated in Figs. 9 and 10, respectively at a/h=10, gradient index n=1, and porosity coefficient ξ=0.2. As we see in Fig. 9, increasing the temperature difference will decrease critical buckling temperature of the porous nanoplate. Also, it is evident from the Fig. 10 that the critical buckling temperature becomes smaller as the moisture difference increases for all nonlocal and strain gradient length scale parameters. Furthermore, from Figs. 9 and 10 it is observed that inclusion of nonlocal and strain gradient length scale parameters have stiffness-softening and stiffness-hardening impact on the porous nanoplate structure. It is also seen that critical buckling temperature of the nanoplate is significantly affected by the moisture and temperature differences.

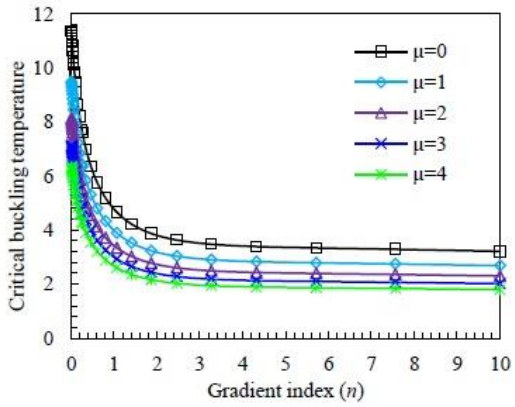

Fig. 7 Influence of gradient index and nonlocal parameter on critical buckling temperature of FG nanoplate λ=0.2

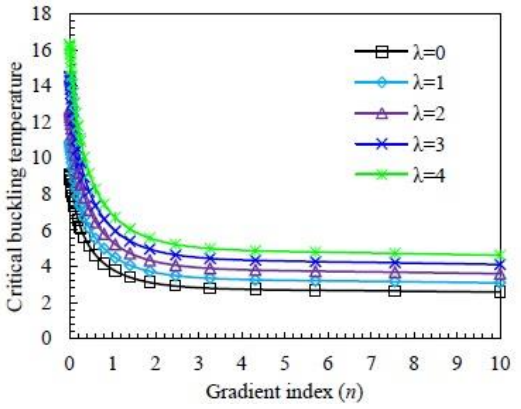

Fig. 8 Influence of gradient index and strain gradient length scale parameter on critical buckling temperature of FG nanoplate μ=1

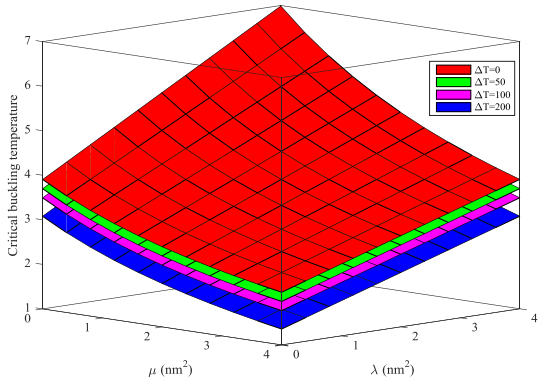

Fig. 9 Effect of temperature difference on critical buckling temperature of FG nanoplate with respect to nonlocal and strain gradient length scale parameters

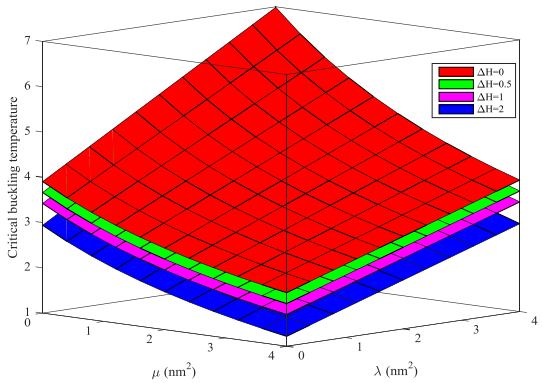

Fig. 10 Effect of humidity difference on critical buckling temperature of FG nanoplate with respect to nonlocal and strain gradient length scale parameters

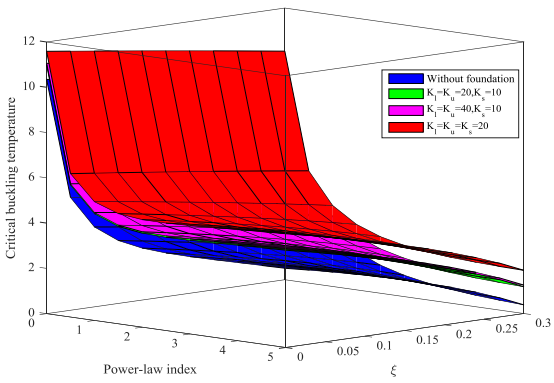

Fig. 11 Effect of elastic Kerr foundation parameters on critical buckling temperature of FG nanoplate with respect to gradient index parameter and porosity coefficient

To better understanding of the foundation's effect, variations of critical buckling temperature of porous nanoplate on an elastic Kerr foundation with respect to gradient index n and porosity coefficient ξ for different Kerr foundation parameters are illustrated in Fig. 11 when a/h=10, μ=1, λ=0.2, ΔT=20, and ΔH=0.5. To simplify the issue, it is assumed that stiffness of upper and lower springs of Kerr foundation are identical. Increasing in stiffness of springs yields increment in the critical buckling temperature. In fact, the porous nanoplate becomes more rigid by increase of springs stiffness leading. Also, it is seen that the presence of shear layer of foundation provides a continuous interaction with the nanoplate and raises the critical buckling temperature. Therefore, the Kerr foundation causes to increase in critical buckling temperature of porous nanoplate, as it has been discussed in several other types of research in the literature. In addition, it is seen that the linear layer parameters possess less influences on the thermal stability in comparison with the shear layer of this foundation.

6. Conclusions

The present work deals adequately with size-dependent thermal stability analysis of sandwich piezoelectric nanoplates with porous core based on a four-variable refined plate theory in conjunction with NSGT under hygrothermal loading. The model contains two different length scale parameters to consider the size-dependent behavior of nanostructures. The porosity and temperature-dependent material properties of porous nanoplate are estimated using a modified power-law rule. The Galerkin method is applied to solve the governing equations derived from Hamilton's principle. As previously specified, gradient index, porosity coefficient, nonlocal and strain gradient parameters, geometry parameters, external voltage, environmental conditions, and Kerr elastic foundation parameters dramatically vary the critical buckling temperature of sandwich porous nanoplate. It is evident that swindling external voltage cause to lower critical buckling temperature. The inclusion of the nonlocal parameter reduces the critical buckling temperature of sandwich nanoplate. Furthermore, the inclusion of the strain gradient length scale parameter improves the nanoplate stiffness as well as critical buckling temperature. Therefore, NSGT provides larger critical buckling temperature when it is compared to NET by introducing a strain gradient length scale parameter. Moreover, it is easily observable that effect of nonlocal parameter and strain gradient length scale parameter on sandwich nanoplates with higher aspect ratios is more considerable than sandwich nanoplates with lower ones.

References

Adpakpang, K., Patil, S.B., Oh, S.M., Kang, J.H., Lacroix, M. and Hwang, S.J. (2016), "Effective chemical route to 2D nanostructured silicon electrode material: phase transition from exfoliated clay nanosheet to porous Si nanoplate", *Electrochimica Acta*, **204**, 60-68.

Atmane, H.A., Tounsi, A., Bernard, F. and Mahmoud, S. (2015), "A computational shear displacement model for vibrational analysis of functionally graded beams with porosities", *Steel Compos. Struct.*, **19**(2), 369-384.

Barati, M., Sadr, M. and Zenkour, A. (2016), "Buckling analysis of higher order graded smart piezoelectric plates with porosities resting on elastic foundation", *Int. J. Mech. Sci.*, **117**, 309-320.

Barati, M.R. (2017a), "Nonlocal-strain gradient forced vibration analysis of metal foam nanoplates with uniform and graded porosities", *Adv. Nano Res.*, **5**(4), 393-414.

Barati, M.R. (2017b), "On wave propagation in nanoporous materials", *Int. J. Eng. Sci.*, **116**, 1-11.

Barati, M.R. (2017c), "Vibration analysis of FG nanoplates with nanovoids on viscoelastic substrate under hygro-thermo-mechanical loading using nonlocal strain gradient theory", *Struct. Eng, Mech.*, **64**(6), 683-693.

Barati, M.R. (2018), "A general nonlocal stress-strain gradient theory for forced vibration analysis of heterogeneous porous nanoplates", Eur. J. Mech. -A/Solids, **67**, 215-230.

Belkorissat, I., Houari, M.S.A., Tounsi, A., Bedia, E. and Mahmoud, S. (2015), "On vibration properties of functionally graded nano-plate using a new nonlocal refined four variable model", *Steel Compos. Struct.*, **18**(4), 1063-1081.

Bellifa, H., Benrahou, K.H., Bousahla, A.A., Tounsi, A. and Mahmoud, S. (2017), "A nonlocal zeroth-order shear deformation theory for nonlinear postbuckling of nanobeams", *Struct. Eng. Mech.*, **62**(6), 695-702.

Bouafia, K., Kaci, A., Houari, M.S.A., Benzair, A. and Tounsi, A. (2017), "A nonlocal quasi-3D theory for bending and free flexural vibration behaviors of functionally graded nanobeams", *Smart Struct. Syst.*, **19**(2), 115-126.

Bounouara, F., Benrahou, K. H., Belkorissat, I. and Tounsi, A. (2016), "A nonlocal zeroth-order shear deformation theory for free vibration of functionally graded nanoscale plates resting on elastic foundation", *Steel Compos. Struct.*, **20**(2), 227-249.

Chaht, F.L., Kaci, A., Houari, M.S.A., Tounsi, A., Bég, O.A. and Mahmoud, S. (2015), "Bending and buckling analyses of functionally graded material (FGM) size-dependent nanoscale beams including the thickness stretching effect", *Steel Compos. Struct.*, **18**(2), 425-442.

Ebrahimi, F. and Daman, M. (2017), "Dynamic characteristics of curved inhomogeneous nonlocal porous beams in thermal environment", *Struct. Eng. Mech.*, **64**(1), 121-133.

Ebrahimi, F. and Salari, E. (2017), "Semi-analytical vibration analysis of functionally graded size-dependent nanobeams with various boundary conditions", *Smart Struct. Syst.*, **19**(3), 243-257.

Ebrahimi, F., Daman, M. and Jafari, A. (2017), "Nonlocal strain gradient-based vibration analysis of embedded curved porous piezoelectric nano-beams in thermal environment", *Smart Struct. Syst.*, **20**(6), 709-728.

Eringen, A.C. and Edelen, D. (1972), "On nonlocal elasticity", *Int. J. Eng. Sci.*, **10**(3), 233-248.

Farajpour, A., Ghayesh, M.H. and Farokhi, H. (2018), "Large-amplitude coupled scale-dependent behaviour of geometrically imperfect NSGT nanotubes", *Int. J. Mech. Sci.*, **150**, 510-525.

Ghadiri, M., Shafiei, N. and Babaei, R. (2017), "Vibration of a rotary FG plate with consideration of thermal and Coriolis effects", *Steel Compos. Struct.*, **25**(2), 197-207.

Ghayesh, M.H. and Farokhi, H. (2017), "Global dynamics of imperfect axially forced microbeams", *Int. J. Eng. Sci.*, **115**, 102-116.

Ghayesh, M.H., Farokhi, H. and Gholipour, A. (2017a), "Oscillations of functionally graded microbeams", *Int. J. Eng. Sci.*, **110**, 35-53.

Ghayesh, M.H., Farokhi, H., Gholipour, A. and Tavallaeinejad, M.

(2017c), "Nonlinear bending and forced vibrations of axially functionally graded tapered microbeams", *Int. J. Eng. Sci*., **120**, 51-62.

Ghayesh, M.H., Farokhi, H., Gholipour, A., Hussain, S. and Arjomandi, M. (2017b), "Resonance responses of geometrically imperfect functionally graded extensible microbeams", J. *Comput. Nonlinear Dynam*., **12**(5), 051002.

Hadji, L. (2017), "Analysis of functionally graded plates using a sinusoidal shear deformation theory", *Smart Struct. Syst*., **19** (4), 441-448.

Jandaghian, A.A. and Rahmani, O. (2017), "Vibration analysis of FG nanobeams based on third-order shear deformation theory under various boundary conditions", *Steel Compos. Struct*., **25** (1), 67-78.

Kaghazian, A., Hajnayeb, A. and Foruzande, H. (2017), "Free vibration analysis of a piezoelectric nanobeam using nonlocal elasticity theory", *Struct. Eng. Mech*., **61**(5), 617-624.

Kar, V.R. and Panda, S.K. (2015), "Nonlinear flexural vibration of shear deformable functionally graded spherical shell panel", *Steel Compos. Struct*., **18**(3), 693-709.

Karami, B. and Janghorban, M. (2016), "Effect of magnetic field on the wave propagation in nanoplates based on strain gradient theory with one parameter and two-variable refined plate theory", *Modern Phys. Lett. B*, **30**(36), 1650421.

Karami, B. and Janghorban, M. (2019), "On the dynamics of porous nanotubes with variable material properties and variable thickness", *Int. J. Eng. Sci*., **136**, 53-66.

Karami, B. and Karami, S. (2019), "Buckling analysis of nanoplate-type temperature-dependent heterogeneous materials", *Adv. Nano Res*., **7**(1), 51-61.

Karami, B., Janghorban, M. and Li, L. (2018a), "On guided wave propagation in fully clamped porous functionally graded nanoplates", *Acta Astronautica*, **143**, 380-390.

Karami, B., Janghorban, M. and Tounsi, A. (2017), "Effects of triaxial magnetic field on the anisotropic nanoplates", *Steel Compos. Struct*., **25**(3), 361-374.

Karami, B., Janghorban, M. and Tounsi, A. (2018c), "Galerkin's approach for buckling analysis of functionally graded anisotropic nanoplates/different boundary conditions", Engineering with Computers.

Karami, B., Janghorban, M. and Tounsi, A. (2018d), "Nonlocal strain gradient 3D elasticity theory for anisotropic spherical nanoparticles", *Steel Compos. Struct*., **27**(2), 201-216.

Karami, B., Janghorban, M. and Tounsi, A. (2018e), "Variational approach for wave dispersion in anisotropic doubly-curved nanoshells based on a new nonlocal strain gradient higher order shell theory", *Thin-Wall. Struct*., **129**, 251-264.

Karami, B., janghorban, M. and Tounsi, A. (2019a), "On exact wave propagation analysis of triclinic material using three-dimensional bi-Helmholtz gradient plate model", *Struct. Eng. Mech*., **69**(5), 487-497.

Karami, B., Janghorban, M., Shahsavari, D. and Tounsi, A. (2018b), "A size-dependent quasi-3D model for wave dispersion analysis of FG nanoplates", *Steel Compos. Struct*., **28**(1), 99-110.

Karami, B., Shahsavari, D. and Janghorban, M. (2018f), "A comprehensive analytical study on functionally graded carbon nanotube-reinforced composite plates", *Aerosp. Sci. Technol*., **82**, 499-512.

Karami, B., Shahsavari, D. and Janghorban, M. (2018g), "Wave propagation analysis in functionally graded (FG) nanoplates under in-plane magnetic field based on nonlocal strain gradient theory and four variable refined plate theory", *Mech. Adv. Mater. Struct*., **25**(12), 1047-1057.

Karami, B., Shahsavari, D. and Li, L. (2018j), "Hygrothermal wave propagation in viscoelastic graphene under in-plane magnetic field based on nonlocal strain gradient theory", *Physica E: Low-dimensional Systems and Nanostructures*, **97**, 317-327.

Karami, B., Shahsavari, D. and Li, L. (2018k), "Temperature-dependent flexural wave propagation in nanoplate-type porous heterogenous material subjected to in-plane magnetic field", *J. Therm. Stresses*, **41**(4), 483-499.

Karami, B., Shahsavari, D., Janghorban, M. and Li, L. (2018h), "Wave dispersion of mounted graphene with initial stress", *Thin-Wall. Struct*., **122**, 102-111.

Karami, B., shahsavari, D., janghorban, M. and Li, L. (2019b), "Influence of homogenization schemes on vibration of functionally graded curved microbeams", *Compos. Struct.*, **216**, 67-79.

Karami, B., Shahsavari, D., Janghorban, M., Dimitri, R. and Tornabene, F. (2019b), "Wave Propagation of Porous Nanoshells", *Nanomaterials*, **9**(1), 22.

Karami, B., Shahsavari, D., Karami, M. and Li, L. (2018i), "Hygrothermal wave characteristic of nanobeam-type inhomogeneous materials with porosity under magnetic field", *Proceedings of the Institution of Mechanical Engineers*, Part C: Journal of Mechanical Engineering Science.

Karami, B., Shahsavari, D., Li, L., Karami, M. and Janghorban, M. (2019d), "Thermal buckling of embedded sandwich piezoelectric nanoplates with functionally graded core by a nonlocal second-order shear deformation theory", *Proceedings of the Institution of Mechanical Engineers, Part C: Journal of Mechanical Engineering Science*, **233**(1), 287-301.

Karami, B., Shahsavari, D., Nazemosadat, S.M.R., Li, L. and Ebrahimi, A. (2018l), "Thermal buckling of smart porous functionally graded nanobeam rested on Kerr foundation", *Steel Compos. Struct*., **29**(3), 349-362.

Khetir, H., Bouiadjra, M.B., Houari, M.S.A., Tounsi, A. and Mahmoud, S. (2017), "A new nonlocal trigonometric shear deformation theory for thermal buckling analysis of embedded nanosize FG plates", *Struct. Eng. Mech*., **64**(4), 391-402.

Kneifati, M. C. (1985), "Analysis of plates on a Kerr foundation model", *J. Eng. Mech*., **111**(11), 1325-1342.

Lam, D.C., Yang, F., Chong, A., Wang, J. and Tong, P. (2003), "Experiments and theory in strain gradient elasticity", *J. Mech. Phys. Solids*, **51**(8), 1477-1508.

Lee, C.Y. and Kim, J.H. (2013), "Hygrothermal postbuckling behavior of functionally graded plates", *Compos. Struct*., **95**, 278-282.

Li, L. and Hu, Y. (2015), "Buckling analysis of size-dependent nonlinear beams based on a nonlocal strain gradient theory", *Int. J. Eng. Sci*., **97**, 84-94.

Li, Q., Iu, V. and Kou, K. (2008), "Three-dimensional vibration analysis of functionally graded material sandwich plates", *J. Sound Vib*., **311**(1-2), 498-515.

Lim, C., Zhang, G. and Reddy, J. (2015), "A higher-order nonlocal elasticity and strain gradient theory and its applications in wave propagation", *J. Mech. Phys. Solids*, **78**, 298-313.

Lü, C., Chen, W. and Lim, C.W. (2009), "Elastic mechanical behavior of nano-scaled FGM films incorporating surface energies", *Compos. Sci. Technol*., **69**(7-8), 1124-1130.

Mechab, I., Mechab, B., Benaissa, S., Serier, B. and Bouiadjra, B. B. (2016), "Free vibration analysis of FGM nanoplate with porosities resting on Winkler Pasternak elastic foundations based on two-variable refined plate theories", *J. Braz. Soc. Mech. Sci. Eng*., **38**(8), 2193-2211.

Nami, M.R. and Janghorban, M. (2014), "Resonance behavior of FG rectangular micro/nano plate based on nonlocal elasticity theory and strain gradient theory with one gradient constant", *Compos. Struct*., **111**, 349-353.

Nejad, M.Z. and Hadi, A. (2016), "Non-local analysis of free vibration of bi-directional functionally graded Euler–Bernoulli nano-beams", *Int. J. Eng. Sci*., **105**, 1-11.

Nejad, M.Z., Hadi, A. and Rastgoo, A. (2016), "Buckling analysis of arbitrary two-directional functionally graded Euler–Bernoulli nano-beams based on nonlocal elasticity theory", *Int. J. Eng. Sci.*, **103**, 1-10.

Rahmani, O., Refaeinejad, V. and Hosseini, S. (2017), "Assessment of various nonlocal higher order theories for the bending and buckling behavior of functionally graded nanobeams", *Steel Compos. Struct.*, **23**(3), 339-350.

Saadatfar, M. and Aghaie-Khafri, M. (2015), "Electromagnetothermoelastic behavior of a rotating imperfect hybrid functionally graded hollow cylinder", *Smart Struct. Syst.*, **15(**6), 1411-1437.

Sedighi, H.M., Daneshmand, F. and Abadyan, M. (2015a), "Modified model for instability analysis of symmetric FGM double-sided nano-bridge: corrections due to surface layer, finite conductivity and size effect", *Compos. Struct.*, **132**, 545-557.

Sedighi, H.M., Keivani, M. and Abadyan, M. (2015b), "Modified continuum model for stability analysis of asymmetric FGM double-sided NEMS: corrections due to finite conductivity, surface energy and nonlocal effect", *Compos. Part B: Eng.*, **83**, 117-133.

Shafiei, N. and She, G.L. (2018), "On vibration of functionally graded nano-tubes in the thermal environment", *Int. J. Eng. Sci.*, **133**, 84-98.

Shahsavari, D. and Janghorban, M. (2017), "Bending and shearing responses for dynamic analysis of single-layer graphene sheets under moving load", *J. Braz. Soc. Mech. Sci. Eng.*, **39**(10), 3849-3861.

Shahsavari, D., Karami, B. and Li, L. (2018b), "Damped vibration of a graphene sheet using a higher-order nonlocal strain-gradient Kirchhoff plate model", *Comptes Rendus Mécanique*, **346**(12), 1216-1232.

Shahsavari, D., Karami, B. and Li, L. (2018c), "A high-order gradient model for wave propagation analysis of porous FG nanoplates", *Steel Compos. Struct.*, **29**(1), 53-66.

Shahsavari, D., Karami, B. and Mansouri, S. (2018d), "Shear buckling of single layer graphene sheets in hygrothermal environment resting on elastic foundation based on different nonlocal strain gradient theories", *Eur. J. Mech.-A/Solids*, **67**, 200-214.

Shahsavari, D., Karami, B., Fahham, H.R. and Li, L. (2018a), "On the shear buckling of porous nanoplates using a new size-dependent quasi-3D shear deformation theory", *Acta Mechanica*, **229**(11), 4549-4573.

Shahsavari, D., Karami, B., Janghorban, M. and Li, L. (2017), "Dynamic characteristics of viscoelastic nanoplates under moving load embedded within visco-Pasternak substrate and hygrothermal environment", *Mater. Res. Express*, **4**(8), 085013.

Shahsavari, D., Shahsavari, M., Li, L. and Karami, B. (2018e), "A novel quasi-3D hyperbolic theory for free vibration of FG plates with porosities resting on Winkler/Pasternak/Kerr foundation", *Aerosp. Sci. Technol.*, **72**, 134-149.

She, G.L., Ren, Y.R., Yuan, F.G. and Xiao, W.S. (2018a), "On vibrations of porous nanotubes", *Int. J. Eng. Sci.*, **125**, 23-35.

She, G.L., Yan, K.M., Zhang, Y.L., Liu, H.B. and Ren, Y.R. (2018b), "Wave propagation of functionally graded porous nanobeams based on non-local strain gradient theory", *Eur. Phys. J. Plus*, **133**(9), 368.

She, G.L., Yuan, F.G. and Ren, Y.R. (2018c), "On wave propagation of porous nanotubes", *Int. J. Eng. Sci.*, **130**, 62-74.

She, G.L., Yuan, F.G., Karami, B., Ren, Y.R. and Xiao, W.S. (2019), "On nonlinear bending behavior of FG porous curved nanotubes", *Int. J. Eng. Sci.*, **135**, 58-74.

She, G.L., Yuan, F.G., Ren, Y.R. and Xiao, W.S. (2017), "On buckling and postbuckling behavior of nanotubes", Int. J. Eng. Sci., **121**, 130-142.

She, G.L., Yuan, F.G., Ren, Y.R., Liu, H.B. and Xiao, W.S. (2018d), "Nonlinear bending and vibration analysis of functionally graded porous tubes via a nonlocal strain gradient theory", *Compos. Struct.*, **203**, 614-623.

Shimpi, R.P. (2002), "Refined plate theory and its variants", *AIAA J.*, **40**(1), 137-146.

Şimşek, M. (2016), "Nonlinear free vibration of a functionally graded nanobeam using nonlocal strain gradient theory and a novel Hamiltonian approach", *Int. J. Eng. Sci.*, **105**, 12-27.

Sobhy, M. (2016), "An accurate shear deformation theory for vibration and buckling of FGM sandwich plates in hygrothermal environment", *Int. J. Mech. Sci.*, **110**, 62-77.

Sobhy, M. (2017), "Hygro-thermo-mechanical vibration and buckling of exponentially graded nanoplates resting on elastic foundations via nonlocal elasticity theory", *Struct. Eng. Mech.*, **63**(3), 401-415.

Wattanasakulpong, N. and Ungbhakorn, V. (2014), "Linear and nonlinear vibration analysis of elastically restrained ends FGM beams with porosities", *Aerosp. Sci. Technol.*, **32**(1), 111-120.

Xiong, Q.L.. and Tian, X. (2017), "Transient thermo-piezo-elastic responses of a functionally graded piezoelectric plate under thermal shock", *Steel Compos. Struct.*, **25**(2), 187-196.

Yu, J.C., Xu, A., Zhang, L., Song, R. and Wu, L. (2004), "Synthesis and characterization of porous magnesium hydroxide and oxide nanoplates", *J. Phys. Chem. B*, **108**(1), 64-70.

Zhang, T. and Shi, Z. (2010), "Exact analyses for two kinds of piezoelectric hollow cylinders with graded properties", *Smart Struct. Syst.*, **6**(8), 975-989.

CC